Urocortin 2 modulates glucose utilization and insulin sensitivity in skeletal muscle

Alon Chen*†, Bhawanjit Brar*, Cheol Soo Choi‡, David Rousso*, Joan Vaughan*, Yael Kuperman†, Shee Ne Kim‡, Cindy Donaldson*, Sean M. Smith*, Pauline Jamieson*, Chien Li*, Tim R. Nagy§, Gerald I. Shulman‡, Kuo-Fen Lee*, and Wylie Vale*¶

*Clayton Foundation Laboratories for Peptide Biology, The Salk Institute for Biological Studies, La Jolla, CA 92037; †Department of Neurobiology, The Weizmann Institute of Science, Rehovot 76100, Israel; ‡Department of Internal Medicine and Cellular and Molecular Physiology and Howard Hughes Medical Institute, Yale University School of Medicine, New Haven, CT 06536; and §Department of Nutrition Sciences, University of Alabama at Birmingham, Birmingham, AL 35294

Contributed by Wylie Vale, August 28, 2006

Skeletal muscle is the principal tissue responsible for insulin-stimulated glucose disposal and is a major site of peripheral insulin resistance. Urocortin 2 (Ucn 2), a member of the corticotropin-releasing factor (CRF) family, and its cognate type 2 CRF receptor (CRFR2) are highly expressed in skeletal muscle. To determine the physiological role of Ucn 2, we generated mice that are deficient in this peptide. Using glucose-tolerance tests (GTTs), insulin-tolerance tests (ITTs), and hyperinsulinemic euglycemic glucose clamp studies, we demonstrated that mice lacking Ucn 2 exhibited increased insulin sensitivity and were protected against fat-induced insulin resistance. Administration of synthetic Ucn 2 to mutant mice before the GTTs and ITTs restored blood glucose to WT levels. Administration of a CRFR2 selective antagonist to WT mice resulted in a GTT profile that mirrored that of Ucn 2-null mice. Body composition measurements of Ucn 2-null mice on a high-fat diet demonstrated decreases in fat and increases in lean tissue compared with WT mice. We propose that null mutant mice display increased glucose uptake in skeletal muscle through the removal of Ucn 2-mediated inhibition of insulin signaling. In keeping with these data, Ucn 2 inhibited insulin-induced Akt and ERK1/2 phosphorylation in cultured skeletal muscle cells and C2C12 myotubes. These data are consistent with the hypothesis that Ucn 2 functions as a local negative regulator of glucose uptake in skeletal muscle and encourage exploration of the possibility that suppression of the Ucn 2/CRFR2 pathway may provide benefits in insulin-resistant states such as type 2 diabetes.

corticotropin-releasing factor | type 2 diabetes | urocortin 2 knockout | glucose homeostasis

Insulin resistance is a characteristic feature in the pathogenesis of type 2 diabetes and obesity (1–4). Although the molecular mechanisms causing this disease are not fully understood, impaired whole-body glucose uptake due to insulin resistance plays a significant role (5–7). Skeletal muscle constitutes the largest insulin-sensitive tissue in humans, and, thus, insulin resistance in this organ impacts whole-body glucose homeostasis (8, 9). Although major advances have been made in our understanding of the molecular mechanisms of insulin action in muscle, little is known of local muscle factors that can modulate insulin action and glucose transport. The neuropeptide corticotropin-releasing factor (CRF) is a key regulator of the hypothalamic–pituitary–adrenal axis under basal and stress conditions (10, 11) and integrates endocrine, autonomic, and behavioral responses to stressors (12–14). It has been suggested that the CRF family peptides and their cognate receptors play a role in modulating energy homeostasis (15–18). Urocortin 2 (Ucn 2, also known as stresscopin-related peptide), a recently identified member of the CRF family (19–21), and its high-affinity, membrane-bound type 2 CRF receptor (CRFR2) (22–25) are highly expressed in skeletal muscle (21–23); however, the physiological functions of Ucn 2 and CRFR2 in this tissue are not known.

Results and Discussion

Generation of Ucn 2-Deficient Mice. To explore the physiological role of Ucn 2, we generated mice that are deficient in this peptide. A genomic DNA clone containing Ucn 2 was isolated, and a targeting construct in which the full Ucn 2 coding sequence was replaced with a neomycin-resistant gene cassette was generated (Fig. 1*a*). J1 ES cells were electroporated with the targeting construct and were selected as described in ref. 26. Targeted ES cells were injected into C57BL/6 mice blastocysts to generate chimeric mice, which transmitted the null mutation through the germ line. Germ-line transmission of the disrupted allele was confirmed by Southern blot analysis by using a 3′ probe (probe A) or 5′ probe (probe B) (Fig. 1*b*). We carried out RT-PCR, RIA, and immunohistochemical staining and determined that Ucn 2 mRNA (Fig. 1*c*) and peptide (Fig. 1 *d* and *e*) were not detected in Ucn 2 mutant mice, demonstrating that disruption of Ucn 2 resulted in a null mutation. Mutant mice are fertile, and the mutant allele was transmitted in a Mendelian fashion.

Metabolic Phenotype of Ucn 2-Null Mice. The ability of the Ucn 2-null mice and their WT littermates to handle a glucose load was assessed by using a standard glucose-tolerance test (GTT). Glucose tolerance was significantly enhanced in the mutant mice compared with their WT littermates (Fig. 2*a*). Administration of synthetic Ucn 2 peptide to mutant mice before the GTT restored blood glucose to WT levels (Fig. 2*b*). Accordingly, administration of the CRFR2 selective antagonist astressin 2B (27) to WT mice resulted in a GTT profile that mirrors that of Ucn 2-null mice (Fig. 2*c*). Fasting basal and glucose-induced elevated insulin levels were similar in the two groups (Fig. 2*d*), suggesting that enhanced glucose tolerance in Ucn 2-null mice is not due to increased insulin secretion into the bloodstream. Ucn 2-null mice demonstrated increased insulin sensitivity compared with their WT littermates as determined by an insulin-tolerance test (ITT) (Fig. 2*e*). Administration of synthetic Ucn 2 peptide to null mutant mice before the ITT restored blood glucose levels to those of WT mice (Fig. 2*f*).

Author contributions: A.C., T.R.N., G.I.S., K.-F.L., and W.V. designed research; A.C., B.B., C.S.C., D.R., J.V., Y.K., S.N.K., C.D., S.M.S., P.J., C.L., and T.R.N. performed research; A.C., B.B., and C.S.C. analyzed data; and A.C. wrote the paper.

Conflict of interest statement: W.V. is a cofounder, consultant, equity holder, and member of the Board of Directors of Neurocrine Biosciences and Acceleron Pharma. The following have been licensed by The Salk Institute for Biological Studies and/or the Clayton Foundation: CRF (to Ferring Pharmaceuticals) and CRF receptors and urocortin 2 (to Neurocrine Biosciences).

Abbreviations: Ucn 2, urocortin 2; CRF, corticotropin-releasing factor; CRFR2, type 2 CRF receptor; GTT, glucose-tolerance test; ITT, insulin-tolerance test.

¶To whom correspondence should be addressed at: Clayton Foundation Laboratories for Peptide Biology, The Salk Institute for Biological Studies, 10010 North Torrey Pines Road, La Jolla, CA 92037. E-mail: vale@salk.edu.

www.pnas.org/cgi/doi/10.1073/pnas.0607337103

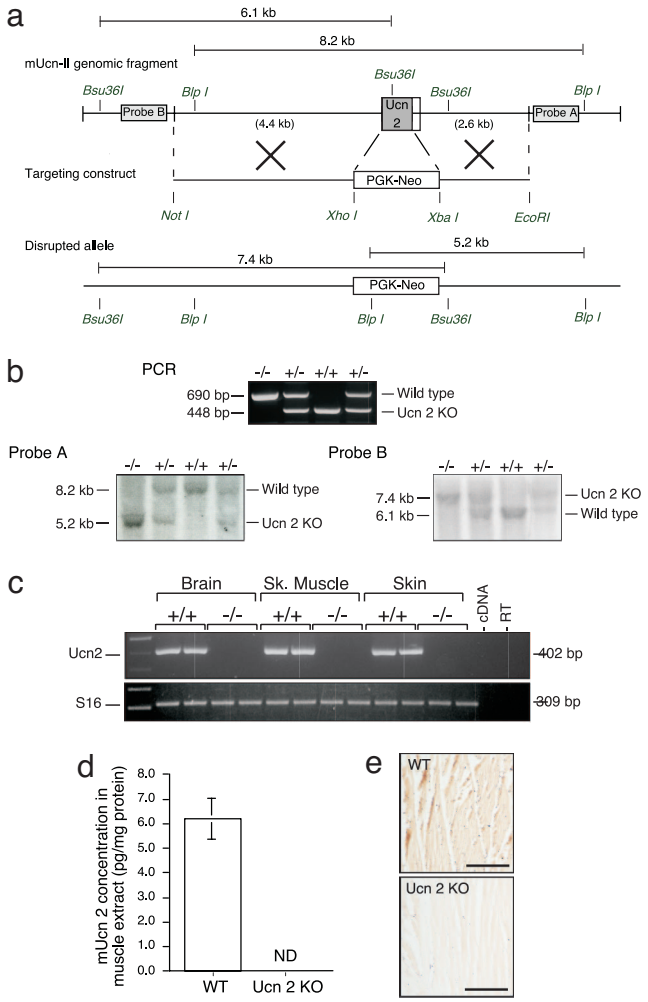

Fig. 1. Generation of Ucn 2-deficient mice. (*a*) Structure of the Ucn 2 gene locus (*Top*), the targeting vector used to transfect ES cells (*Middle*), and the mutated locus (*Bottom*). (*b*) Southern blot analysis and PCR amplification of tail DNA isolated from the progeny of heterozygote crosses (WT, +/+; heterozygous, +/−; null mutant, −/−). (*c*) RT-PCR shows the absence of Ucn 2 mRNA in the brain, skeletal muscle, and skin of the Ucn 2 mutant mice. (*d*) Ucn 2-like immunoreactivity measured by RIA in acid extracts of partially purified skeletal muscle tissue isolated from WT or null mutant mice shows the absence of Ucn 2 peptide in the mutant mice. (*e*) Immunostaining using antisera against Ucn 2 shows the absence of Ucn 2 peptide in paraffin-embedded sections obtained from WT or null mutant mice. KO, knockout.

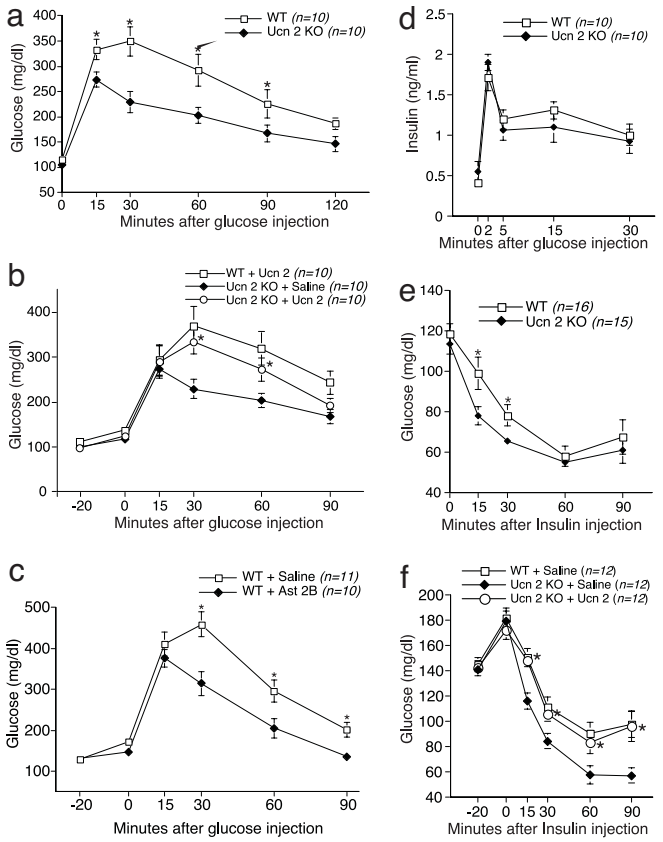

Fig. 2. Metabolic phenotype of Ucn 2-null mice. (*a*) Ucn 2-null mice show enhanced glucose tolerance. The ability of the Ucn 2-null mice and their WT littermates to handle a glucose load was assessed by using a standard GTT. Fasted male mice were injected i.p. with glucose (2 g/kg of body weight), and blood glucose levels were measured before and at 15, 30, 60, 90, and 120 min after glucose injection. (*b*) Administration of synthetic Ucn 2 peptide to mutant mice before the GTT restores blood glucose to WT levels. Fasted male Ucn 2-null mice were injected i.p. with saline or with Ucn 2 (0.1 mg/kg of body weight) 20 min before glucose injection (2 g/kg of body weight), and blood glucose levels were measured before and at 15, 30, 60, and 90 min after glucose injection. (*c*) Administration of the CRFR2-specific antagonist astressin 2B into WT mice mimics the Ucn 2 mutant mice GTT profile. Fasted male WT mice were injected i.p. with saline or with astressin 2B (30 mg/kg of body weight) 20 min before glucose injection (2 g/kg of body weight), and blood glucose levels were measured before and at 15, 30, 60, and 90 min after glucose injection. (*d*) The enhanced glucose tolerance in the Ucn 2-null mice is not due to increased insulin secretion. Fasted male mice were injected i.p. with glucose (3 g/kg of body weight), and blood samples were collected at 2, 5, 15, and 30 min after glucose injection. Insulin was measured by RIA. (*e*) Ucn 2-null mice show increased insulin sensitivity by ITT. Fasted male mice were injected i.p. with insulin (0.75 units/kg of body weight), and blood glucose levels were measured before and at 15, 30, 60, and 90 min after insulin injection. (*f*) Administration of synthetic Ucn 2 peptide to mutant mice before the ITT restores blood glucose to WT levels. Fasted male Ucn 2-null mice were injected i.p. with saline or Ucn 2 peptide (0.1 mg/kg of body weight) 20 min before insulin injection (0.75 units/kg of body weight), and blood glucose levels were measured before and at 15, 30, 60, and 90 min after insulin injection. KO, knockout.

Dynamic Metabolic Studies of Ucn 2-Null Mice. Because insulin tolerance testing assesses glucose disposal after an acute i.p. injection of insulin, we examined whole-body glucose homeostasis by using hyperinsulinemic euglycemic glucose clamp studies. During constant hyperinsulinemia in mice fed a standard chow diet, higher glucose infusion rates were required to maintain normal glucose levels in Ucn 2-null mice compared with their WT littermates (Fig. 3 *a* and *b*). To evaluate the contribution of peripheral tissues to the increased insulin responsiveness, the actions of insulin on liver, fat, and skeletal muscle were measured by using radiolabeled glucose analogues during the clamp studies (Fig. 3 *c–f*). Whole-body glucose uptake (peripheral insulin sensitivity), glycolysis, and insulin-mediated suppression of hepatic glucose production rates (hepatic insulin sensitivity) were significantly increased in the mutant mice compared with WT littermates (Fig. 3 *c* and *d*). An insulin sensitivity index of adipose tissue, measured as suppression of lipolysis, was increased in mutant mice compared with WT littermates (Fig. 3*e*). To assess the effect of the Ucn 2-null mutation on skeletal muscle, we measured specific glucose uptake into the gastrocnemius muscle and found a significant increase of deoxy-[2-^{3}H] glucose uptake in skeletal muscle of mutant mice as compared with WT littermates (Fig. 3*f*). Data from these clamp studies were congruent with our initial observation that Ucn 2-null mice are more insulin sensitive than WT control mice.

PHYSIOLOGY

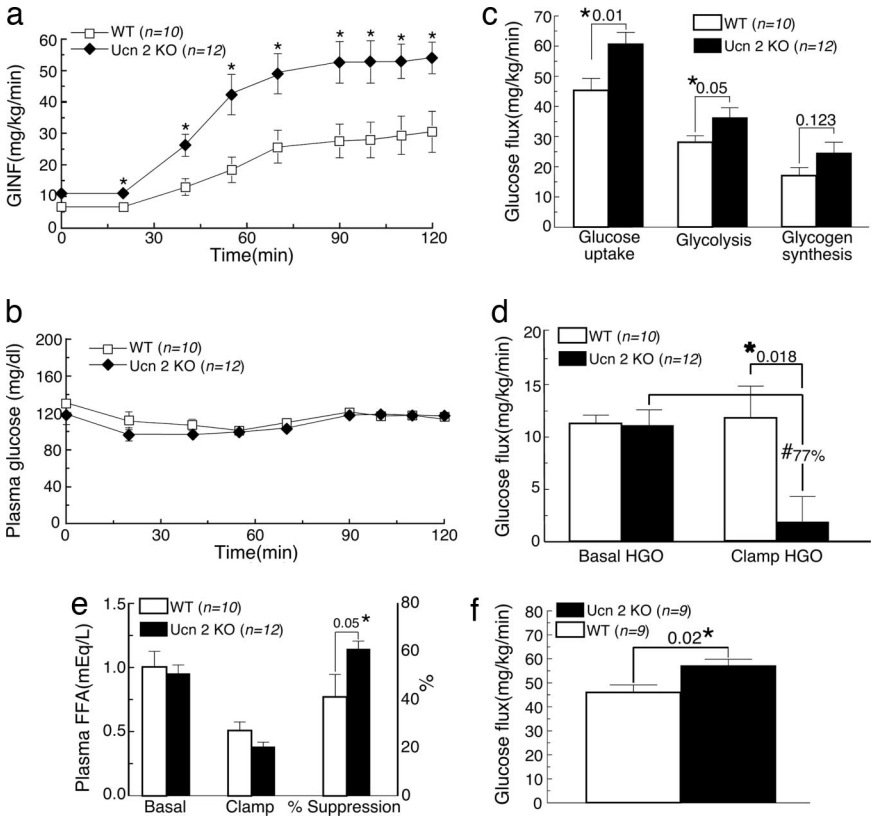

Fig. 3. Dynamic metabolic studies of Ucn 2-null mice. (*a–d*) Hyperinsulinemic euglycemic clamp studies of Ucn 2-null mice and their WT littermates fed a standard chow diet. (*a*) The glucose infusion rate (GINF) required to maintained euglycemia in mutant mice was significantly higher than that of WT littermates. (*b*) Blood glucose levels during the clamp study were maintained at the level of ≈120 mg/dl. (*c* and *d*) Whole-body glucose uptake (peripheral insulin sensitivity, *c*) and insulin-mediated suppression of hepatic glucose production rates (hepatic insulin sensitivity, *d*) are significantly increased in Ucn 2-null mice compared with WT littermates. HGO, hepatic glucose output. (*e*) An insulin sensitivity index of adipose tissue, measured as suppression of lipolysis, was increased in mutant mice compared with WT littermates. (*f*) To assess the effect of a Ucn 2-null mutation on skeletal muscle, we measured specific glucose uptake into the gastrocnemius muscle and found a significant increase of deoxy-[2-^{3}H] glucose uptake in skeletal muscle of mutant mice compared with WT littermates.

Ucn 2-Null Mice Placed on a High-Fat Diet Exhibit Increased Insulin Sensitivity and Are Protected Against Fat-Induced Insulin Resistance. Mice fed a high-fat diet provide a well established model for studying impaired glucose tolerance and ontogeny of type 2 diabetes. To explore glucose metabolism in Ucn 2-null mice, mutant and WT mice were placed on a high-fat (45% of calories from fat) or a standard chow (11% of calories from fat) diet for 16 weeks (Fig. 4 *a–f*). The weight gain (Fig. 4*d*) and food consumed on a standard or high-fat diet (Fig. 4*c*) by the Ucn 2-null mice were similar to those of the WT mice. Remarkably, however, significant increases in blood glucose (Fig. 4*a*) and insulin levels (Fig. 4*b*) were observed in the WT mice but not in Ucn 2-null mice. Body composition measurements determined by using dual-energy x-ray absorptiometry (28) of Ucn 2-null mice on a high-fat diet demonstrated decreases in fat (Fig. 4*e*) and increases in lean tissue (Fig. 4*f*) compared with WT littermates. To assess insulin actions on whole-body, liver, and skeletal muscle tissues, we performed hyperinsulinemic euglycemic clamp studies on both WT and Ucn 2-null mice that were fed a high-fat diet (55% of calories from fat) for 3 weeks (Fig. 4 *g–j*). Ucn 2-null mice on a high-fat diet required higher glucose infusion rates to maintain normal glucose levels in hyperinsulinemic euglycemic glucose clamp studies (Fig. 4 *g* and *h*). Furthermore, whole-body glucose uptake and glycogen synthesis (Fig. 4*i*) and specific glucose uptake by gastrocnemius tissue (Fig. 4*j*) were significantly increased in mutant mice compared with WT littermates. These data demonstrate that mice lacking Ucn 2 have increased glucose utilization and are protected against fat-induced insulin resistance in skeletal muscle.

Ucn 2 Effects on Muscle Glucose Uptake Are Mediated Putatively by Inhibition of Insulin Signaling. The insulin signaling pathways controlling glucose transport into skeletal muscle are complex; multiple effector proteins are believed to orchestrate diverse cellular responses (6, 7, 29). Adding to this complexity, the signaling pathways are not linear, and there is a high degree of cross-talk between the signal transducers. The serine/threonine kinase Akt/PKB plays a key role in insulin signaling, and its activation by insulin has been shown to play a crucial role in the control of GLUT4 (glucose transporter 4) translocation and glycogen metabolism (6, 7, 29). To establish that Ucn 2 can have direct effects on skeletal muscle, we studied the effects of Ucn 2 on insulin signaling in cultured skeletal muscle cells and C2C12 myotubes. Ucn 2 inhibits insulin-induced phosphorylation of Akt in C2C12 myotubes (Fig. 5 *a* and *b*) and in cultured skeletal muscle cells (Fig. 5 *c* and *d*). The inhibitory effect of Ucn 2 and CRFR2 activation on insulin receptor signaling may be mediated early in the signaling cascade, because ERK1/2 phosphorylation after insulin stimulation is also inhibited by Ucn 2 treatment (Fig. 5 *e* and *f*). The β-adrenergic agonist isoproterenol was also previously demonstrated to markedly reduce the increase in ERK1/2 activities produced by insulin in rat adipocytes (30). Ucn 2 inhibits insulin-induced glucose uptake in C2C12 myotubes (Fig. 5*g*). This dose-dependent inhibition is consistent with the inhibition of insulin signaling by Ucn 2. These results suggest that Ucn 2 inhibits interactions between the insulin signaling pathway components. The molecular mechanism by which Ucn 2, acting through its specific G protein-coupled receptor, inhibits insulin receptor signaling remains to be determined.

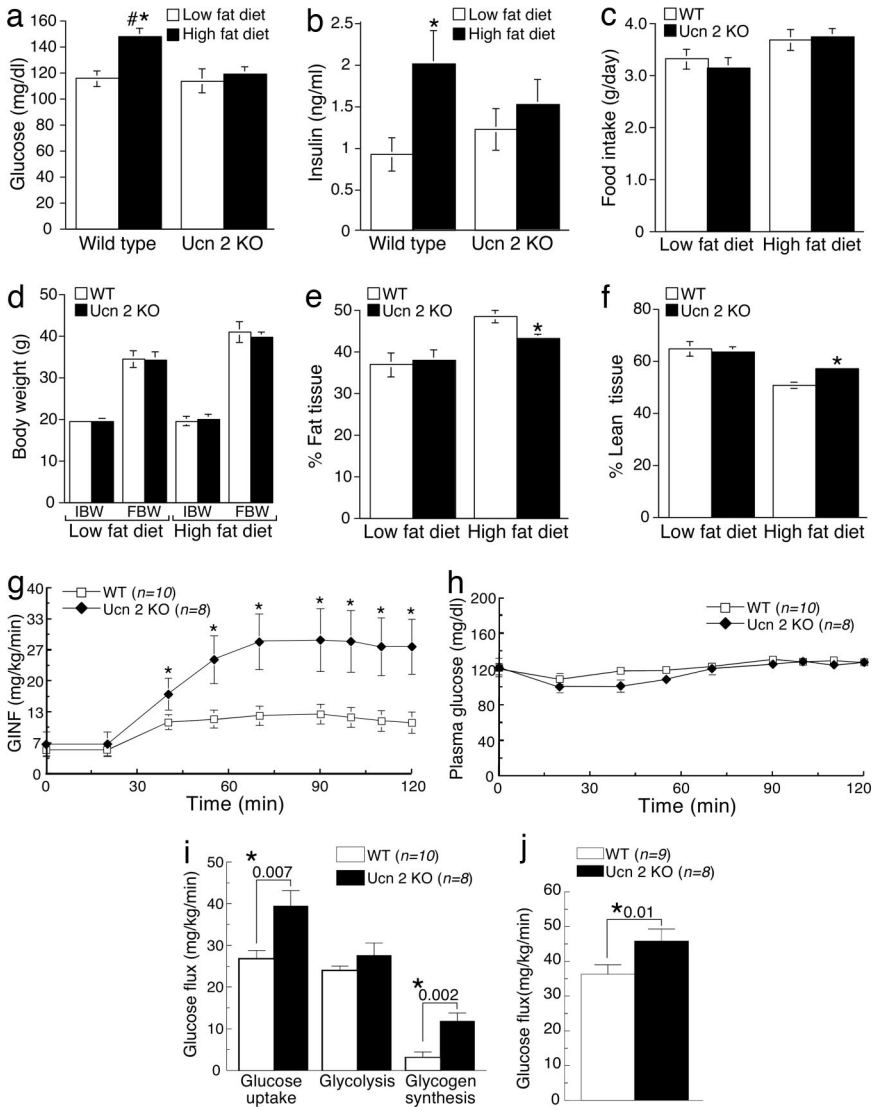

Fig. 4. Ucn 2-null mice placed on a high-fat diet exhibit increased insulin sensitivity and are protected against fat-induced insulin resistance. (*a–f*) Ucn 2-null mice and their WT littermates were placed on a high-fat diet (45% of calories from fat) or standard chow diet (10% of calories from fat) for 16 weeks. Significant increases in blood glucose (*a*) and insulin (*b*) levels were observed in the WT mice but not in Ucn 2-null mice. No differences were observed in food intake (*c*) or body weight (*d*) when comparing mutant and WT mice in the high-fat and low-fat groups. Body composition of Ucn 2-null mice on a high-fat diet shows decreases in fat (*e*) and increases in lean tissue (*f*) compared with WT littermates. (*g–j*) Hyperinsulinemic euglycemic clamp studies of Ucn 2-null mice and their WT littermates maintained on a high-fat diet (55% of calories from fat) for 3 weeks. (*g*) The glucose infusion rate (GINF) required to maintained euglycemia in mutant mice was significantly higher than that of WT littermates. (*h*) Blood glucose levels during the clamp study were maintained at the level of ≈120 mg/dl. (*i* and *j*) Whole-body glucose uptake (peripheral insulin sensitivity, *i*) and specific glucose uptake by the gastrocnemius muscle tissue (*j*) are significantly increased in Ucn 2-null mice compared with WT littermates.

Skeletal muscle accounts for ≈80% of glucose disposal after glucose infusion and is of principal importance in maintaining glucose homeostasis (29, 31). Alterations in signal transduction to glucose transport have a profound effect on whole-body glucose homeostasis (5–9). Ucn 2 and its specific receptor, CRFR2, are highly expressed by skeletal muscle and can serve as an autocrine and/or paracrine regulator of glucose uptake in this tissue. Although the primary defects that are responsible for the development of type 2 diabetes are unclear, insulin resistance in skeletal muscle is a hallmark of the disease (5–9). In normal glucose-tolerant relatives of type 2 diabetic patients, insulin resistance in skeletal muscle has been observed several years before the development of overt diabetes (32, 33). Thus, impaired insulin action in skeletal muscle may constitute an early defect in the pathogenesis of type 2 diabetes. Maintaining glucose homeostasis in the presence of diverse challenges, such as starvation, requires numerous adaptive responses. We have shown that Ucn 2 can regulate glucose utilization by modulating insulin sensitivity in skeletal muscle. Ucn 2, by decreasing glucose uptake in skeletal muscle, may serve an important adaptive function to increase glucose availability for other tissues under specific conditions. Generation of muscle- or brain-specific Ucn 2 knockout mice would facilitate our understanding of the role of central Ucn 2 to the observed phenotype. Our data support a physiological function for Ucn 2 peptide as a local regulator of glucose uptake in muscle and suggest a potential therapeutic use for antagonists of its cognate receptor in the management of type 2 diabetes.

Materials and Methods

Construction of Ucn 2-Null Mice. A genomic DNA clone containing the Ucn 2 gene locus was isolated, and a targeting construct in which

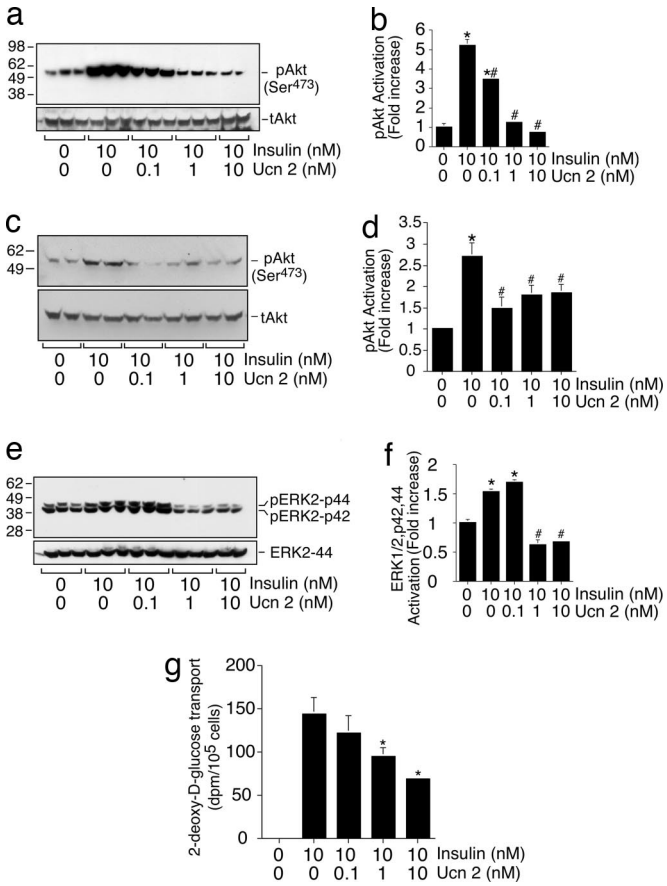

Fig. 5. Ucn 2 effects on muscle glucose uptake are mediated putatively by inhibition of insulin signaling. (*a–f*) Ucn 2 inhibits insulin-induced Akt and ERK1/2 phosphorylation. Differentiated C2C12 myotubes or cultured skeletal muscle cells were preincubated with or without Ucn 2 peptide (0.1, 1, or 10 nM) for 1 h before insulin treatment (10 nM for 5 min). Cell lysates were resolved by using 4–12% gradient polyacrylamide gels. Gels were electrophoretically transferred to membranes and probed with antibodies specific for the phospho proteins pAkt (Ser-473) or pERK1/2. Stimulation of Akt or ERK activation was calculated by fold activation of the phosphorylated form normalized to total and compared with the nontreatment controls (*b*, *d*, and *f*). Ucn 2 dose dependently inhibits the insulin-induced phosphorylation of Akt (*a–d*) and ERK1/2 (*e* and *f*). (*g*) The effect of Ucn 2 on [^{3}H]2-deoxy-D-glucose uptake in differentiated C2C12 myotubes. Cells were incubated for 2 h in low-glucose, serum-free medium and treated with Ucn 2 (0.1, 1, or 10 nM) or without Ucn 2 (control) for 30 min before insulin administration (10 nM). Glucose uptake was measured 5 min after exposure to [^{3}H]2-deoxy-D-glucose. Nonspecific uptake was measured by incubating muscle tissue with cytochalasin B, which binds to the glucose uptake transporter (GLUT) and inhibits glucose transport into the cell. Specific uptake was calculated by subtracting nonspecific glucose from total glucose.

the Ucn 2 coding sequence was replaced with a neomycin-resistant gene cassette was generated. ES cell cultures were established, and positive ES clones were injected into C57BL/6 blastocysts to generate chimeric mice as described in ref. 26. Chimeras were mated to produce heterozygous mutant mice on a mixed C57BL/6 and 129 genetic background. Breeding of these mice was continued and maintained by means of heterozygote × heterozygote nonsibling matings. Mutant mice were fertile, and the mutant allele was transmitted in a Mendelian fashion. All animal protocols were approved by the Salk Institute for Biological Studies Institutional Animal Care and Use Committee. Detailed descriptions of the RNA preparation and semiquantitative RT-PCR, immunohistochemistry, and RIA used to demonstrate the null mutation can be found in the *Supporting Materials and Methods*, which is published as supporting information on the PNAS web site.

GTT, ITT, and Insulin-Release Assay. For the GTT, glucose (2 g/kg of body weight) was injected i.p. after mice were fasted overnight for 14 h. Whole venous blood obtained from the tail vein at 0, 15, 30, 60, 90, and 120 min after the injection was measured for glucose by using an automatic glucometer (One Touch, Lifescan, Daly, CA).

For insulin release, glucose (3 g/kg of body weight) was injected i.p.; blood was collected by retroorbital eye bleed at 0, 2, 5, 15, and 30 min after the injection and immediately centrifuged, and the plasma was stored at −20°C. Insulin levels were measured by using a commercially available RIA kit (Linco, St. Louis, MO).

For the ITT, fasted male mice were injected with insulin (0.75 units/kg of body weight, Sigma, St. Louis, MO), and blood glucose levels were measured before and at 15, 30, 60, and 90 min after insulin injection.

In separate experiments, mice were i.p. injected with saline or Ucn 2 peptide (0.1 mg/kg of body weight) 20 min before the ITT and GTT or with astressin 2B (30 mg/kg of body weight) 20 min before the GTT.

Hyperinsulinemic Euglycemic Clamp Studies. ***Animals.*** Male Ucn 2-null mice and age-matched WT littermates were studied at 16–18 weeks of age. They were placed on a standard lab chow diet or a high-fat diet (55% of calories from fat, diet TD 93075, Harlan Teklad, Indianapolis, IN) for 3 weeks and housed under controlled temperature (22 ± 2°C) and lighting [12-h light (0700–1700) and 12-h dark (1700–0700)] conditions with free access to water and food.

Clamp experiments. At least 6 days before the hyperinsulinemic euglycemic clamp experiments, an indwelling catheter was implanted into the left jugular vein of mice. All procedures were approved by the Yale University Animal Care and Use Committee.

After an overnight fast, [3-^{3}H]glucose (HPLC-purified; PerkinElmer, Boston, MA) was infused at a rate of 0.05 μCi/min (1 Ci = 37 GBq) for 2 h to assess the basal glucose turnover. After the basal period, a hyperinsulinemic euglycemic clamp was conducted for 120 min with a primed and continuous infusion of human insulin (105 pmol/kg for the prime and 15 pmol/kg/min for the infusion) (Novo Nordisk, Princeton, NJ) to raise plasma insulin within the physiological range. Blood samples (10 μl) were collected at 10- to 20-min intervals for the immediate measurement of plasma glucose, and 20% dextrose was infused at variable rates to maintain plasma glucose at basal concentrations (≈6.7 mM). To estimate insulin-stimulated whole-body glucose fluxes, [3-^{3}H]glucose was infused at a rate of 0.1 μCi/min throughout the clamps, and 2-deoxy-D-[1-^{14}C]glucose (PerkinElmer) was injected as a bolus after 75 min of clamping to estimate the rate of insulin-stimulated tissue glucose uptake as described in ref. 32. Blood samples (10 μl) for the measurement of plasma ^{3}H and ^{14}C activities were taken at the end of the basal period and during the last 45 min of the clamp. Additional blood samples were obtained for the measurement of plasma insulin and free fatty acid concentrations at the end of the basal and clamp time period. At the end of the clamp, mice were anesthetized with sodium pentobarbital, and tissues were taken for biochemical measurements within 3 min: three muscles (gastrocnemius, tibialis anterior, and quadriceps) from each hindlimb, epididymal fat, liver brown fat, and heart. Each tissue sample was quickly dissected, frozen immediately by using liquid N_2-cooled aluminum blocks, and stored at −80°C for later analysis. A detailed description of the biochemical analysis and calculations of the hyperinsulinemic euglycemic clamp studies can be found in *Supporting Materials and Methods.*

Body Composition Analysis Using Dual-Energy X-Ray Absorptiometry (DXA). All DXA measurements were conducted by using the GE-Lunar PIXImus (General Electric, Madison, WI) as described and validated in ref. 28. Previously frozen mice were thawed and allowed to reach room temperature before being scanned by using

software version 1.45. The head of the animal was excluded from the analysis by using the exclusion tool provided with the software as we have described in ref. 28. Data were analyzed to determine fat and lean tissue masses and bone mineral content and density.

Glucose Uptake in Cultured Muscle Cells. C2C12 myoblasts were cultured in DMEM supplemented with 10% FBS and 1% (vol/vol) antibiotic solution at 37°C in a 5% CO_2-humidified atmosphere. When subconfluent density was achieved, cells were transferred to differentiation media containing 2% horse serum for 8–10 days, in which time the myoblast cells were fully differentiated to functional myotubes. The C2C12 myotubes were washed once with serum-free DMEM and transferred to low-glucose, serum-free DMEM containing 0.1% BSA for 2 h. After starvation, cells were washed with Hanks' balanced saline solution (HBSS) and incubated with the same buffer for an additional 2 h. To determine the effect of Ucn 2 on insulin-induced glucose uptake, 30-min incubations in HBSS without or with increasing concentrations (0.1, 1, or 10 nM) of Ucn 2 were carried out. Insulin was added at 10 nM concentration directly into the HBSS, and incubation continued for an additional 30 min. The reaction was performed by adding a mixture of [^{3}H]2-deoxyglucose (0.2 mCi/ml) and nonradioactive 2-deoxyglucose (final concentration of 0.1 mM) for 5 min. The solution was removed by suction, and the cells were rapidly washed four times with ice-cold PBS. Radiolabeled glucose was released from the cells by incubating the cells with 1M NaOH for 30 min. An aliquot for the protein assay was taken before neutralizing the sample with 1M HCl. The extract was counted for radioactivity in EcoLume scintillation fluid by using a β-counter. Nonspecific uptake was measured by incubating the cells with cytochalasin B (40 mM/ml; Sigma), which binds to the glucose uptake transporter and inhibits glucose transport into the cell. Nonspecific uptake was subtracted from total uptake to obtain specific uptake values.

Skeletal Myocyte Culture. Skeletal myocytes were isolated from the limbs of neonatal WT mice that were <2 days old. After collagenase digestion, the cells were preplated in medium consisting of DMEM [1,000 μg of glucose/liter/1 mmol/liter L-glutamine/100 units/ml penicillin/streptomycin (all from Life Technologies, Rockville, MD)] supplemented with 15% (vol/vol) FBS on 10-cm tissue culture dishes. Preplating of the cell suspension for 30 min allowed contaminating fibroblasts to attach and the myocytes to remain free in the culture media. Subsequent to this incubation, the myocyte cell suspension was transferred onto 12-well (1 cm) gelatin-coated plates or to 8-well chamber slides. After 24 h in culture, the medium was replaced with medium containing reduced FBS at 1% (vol/vol) for an additional 48 h before being used for experiments.

Analysis of Protein Levels by Western Blotting. Primary mouse skeletal muscle myocytes or differentiated C2C12 myotubes were preincubated with or without Ucn 2 peptide (0.1, 1, or 10 nM) for 1 h before insulin treatment (10 nM for 5 min). Cells were harvested immediately in 100 μl of sample treatment buffer [50 mM Tris, pH 6.8/100 mM DTT/2% (wt/vol) SDS/0.1% (wt/vol) bromophenol blue/10% (wt/vol) glycerol]. The samples were boiled for 5 min, and proteins were electrophoresed on 4–12% SDS-polyacrylamide gradient gel (Invitrogen Life Technologies, Carlsbad, CA), transferred onto nitrocellulose membranes, and probed with antibodies specific for phosphorylated Akt (Ser-473; Cell Signaling Technology, Beverly, MA) or phosphorylated ERK1/2-p42, 44 (Santa Cruz Biotechnology, Santa Cruz, CA). The membranes were washed with PBS containing 0.05% (vol/vol) Tween 20 and incubated with horseradish peroxidase-conjugated anti-mouse or anti-rabbit IgG raised in sheep (Amersham Biotech Amersham Pharmacia, Piscataway, NJ). Immunoreactive proteins were visualized by using Super Signal West Pico Chemiluminescent substrate (Pierce, Rockford, IL). The relative protein levels were determined by using densitometry (Imagequant 1.2) and by probing the membranes with antibodies directed against total proteins.

This work was supported by National Institute of Diabetes and Digestive and Kidney Diseases (NIDDK) Program Project Grant DK 26741, the Robert J. and Helen C. Kleberg Foundation, the Adler Foundation, the Clayton Foundation's Foundation for Research (W.V.), NIDDK Grants DK 40936 and U24 DK 59635 (to G.I.S.), the University of Alabama at Birmingham Clinical Nutrition Research Unit (Grant P30 DK56336 to T.R.N.), and the National Institutes of Health. W.V. is a Senior Foundation for Research Investigator. G.I.S. is the recipient of a Distinguished Clinical Scientist Award from the American Diabetes Association.

1. Spiegelman BM, Flier JS (2001) *Cell* 104:531–543.
2. Friedman JM (2004) *Nat Med* 10:563–569.
3. Bouche C, Serdy S, Kahn CR, Goldfine AB (2004) *Endocr Rev* 25:807–837.
4. Evans RM, Barish GD, Wang YX (2004) *Nat Med* 10:355–361.
5. Seely LB, Olefsky JM (1993) in *Insulin Resistance* (Wiley, New York), pp 187–252.
6. Shulman GI (2000) *J Clin Invest* 106:171–176.
7. Virkamaki A, Ueki K, Kahn CR (1999) *J Clin Invest* 103:931–943.
8. Shulman GI (2004) *Physiology* 19:183–190.
9. Zierath JR, Krook A, Wallberg-Henriksson H (2000) *Diabetologia* 43:821–835.
10. Vale W, Spiess J, Rivier C, Rivier J (1981) *Science* 213:1394–1397.
11. Rivier C, Vale W (1983) *Nature* 305:325–327.
12. Sutton RE, Koob GF, Le Moal M, Rivier J, Vale W (1982) *Nature* 297:331–333.
13. Bale TL, Vale WW (2004) *Annu Rev Pharmacol Toxicol* 44:525–557.
14. Charmandari E, Tsigos C, Chrousos G (2005) *Annu Rev Physiol* 67:259–284.
15. Brown MR, Fisher LA, Spiess J, Rivier C, Rivier J, Vale W (1982) *Endocrinology* 111:928–931.
16. Dallman MF, Akana SF, Strack AM, Hanson ES, Sebastian RJ (1995) *Ann NY Acad Sci* 771:730–742.
17. Bale TL, Anderson KR, Roberts AJ, Lee KF, Nagy TR, Vale WW (2003) *Endocrinology* 144:2580–2587.
18. De Kloet ER (2004) *Ann NY Acad Sci* 1018:1–15.
19. Reyes TM, Lewis K, Perrin MH, Kunitake KS, Vaughan J, Arias CA, Hogenesch JB, Gulyas J, Rivier J, Vale WW, Sawchenko PE (2001) *Proc Natl Acad Sci USA* 98:2843–2848.
20. Hsu SY, Hsueh AJ (2001) *Nat Med* 7:605–611.
21. Chen A, Blount A, Vaughan J, Brar B, Vale W (2004) *Endocrinology* 145:2445–2457.
22. Perrin M, Donaldson C, Chen R, Blount A, Berggren T, Bilezikjian L, Sawchenko P, Vale W (1995) *Proc Natl Acad Sci USA* 92:2969–2973.
23. Kishimoto T, Pearse RV, II, Lin CR, Rosenfeld MG (1995) *Proc Natl Acad Sci USA* 92:1108–1112.
24. Perrin MH, Vale WW (1999) *Ann NY Acad Sci* 885:312–328.
25. Chen A, Perrin M, Brar B, Li C, Jamieson P, Digruccio M, Lewis K, Vale W (2005) *Mol Endocrinol* 19:441–458.
26. Smith GW, Aubry JM, Dellu F, Contarino A, Bilezikjian LM, Gold LH, Chen R, Marchuk Y, Hauser C, Bentley CA, *et al.* (1998) *Neuron* 20:1093–1102.
27. Rivier J, Gulyas J, Kirby D, Low W, Perrin MH, Kunitake K, DiGruccio M, Vaughan J, Reubi JC, Waser B, *et al.* (2002) *J Med Chem* 45:4737–4747.
28. Nagy TR, Clair AL (2000) *Obes Res* 8:392–398.
29. Zierath JR, Wallberg-Henriksson H (2002) *Ann NY Acad Sci* 967:120–134.
30. Sevetson BR, Kong X, Lawrence JC, Jr (1993) *Proc Natl Acad Sci USA* 90:10305–10309.
31. Shulman GI, Rothman DL, Jue T, Stein P, DeFronzo RA, Shulman RG (1990) *N Engl J Med* 322:223–228.
32. Vaag A, Henriksen JE, Beck-Nielsen H (1992) *J Clin Invest* 89:782–788.
33. Warram JH, Martin BC, Krolewski AS, Soeldner JS, Kahn CR (1990) *Ann Intern Med* 113:909–915.